Absolute Rate of Charge Separation and Recombination in a Molecular Model of the P3HT/PCBM Interface

ARTICLE *in* THE JOURNAL OF PHYSICAL CHEMISTRY C · JANUARY 2011

Impact Factor: 4.77 · DOI: 10.1021/jp109130y

THE JOURNAL OF PHYSICAL CHEMISTRY C

ARTICLE

pubs.acs.org/JPCC

Absolute Rate of Charge Separation and Recombination in a Molecular Model of the P3HT/PCBM Interface

Tao Liu* and Alessandro Troisi*

Department of Chemistry and Centre for Scientific Computing, University of Warwick, Coventry, CV4 7AL, United Kingdom

Supporting Information

ABSTRACT: A simplified model system is used to compute the rates of interfacial charge separation (CS) and recombination (CS) in the P3HT/PCBM blend (poly(3-hexylthiophene) and [6,6]-phenyl-C_{61}-butyric acid methyl ester) used in bulk heterojunction solar cells. The absolute charge-transfer rates of CS (k_{CS}) and CR (k_{CR}) processes were calculated to be 1.50×10^{11} and 1.93×10^{9} s^{-1}, respectively, from the Marcus−Levich−Jortner rate equation, in reasonable agreement with the range of available experimental values for a model containing a six thiophene rings chain and a single PCBM molecule. A detailed discussion of the inaccuracy intrinsic in the evaluation of all quantities entering the rate expression (equilibrium energy, electronic coupling, and internal and external reorganization energies) is provided together with a discussion of the sensitivity of the computed rate to these quantities. A variety of DFT methods is used to evaluate the states energy of the system (TDDFT, calculation with background charges, and unrestricted DFT), and it was found that unrestricted calculations of the lowest triplet state can describe with good accuracy the equilibrium energy and geometry of the charge-transfer states. A physically plausible range for the external reorganization energy is computed with a continuum model, and it is shown that a more accurate evaluation of this quantity is not essential.

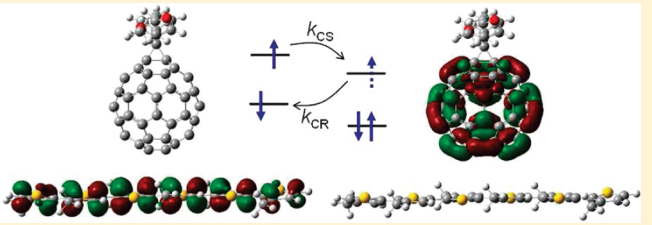

1. INTRODUCTION

The power conversion efficiency (PCE) of the most common solar cell, based on silicon, has almost reached the theoretical limit (29%),[1,2] but the high production cost hinders its wide application. Organic solar cells (OSCs) have attracted much attention in the past few years as a potential low-cost replacement for the silicon photovoltaics and also because of their flexibility, ease of processing, and low toxicity.[2−5] The organic solar cells made by a regioregular poly(3-hexylthiophene) (P3HT) as donor and [6,6]-phenyl-C_{61}-butyric acid methyl ester (PCBM) as acceptor in bulk heterojonction have been widely investigated experimentally and theoretically and are the main reference system for this class of devices.[3,6−12] The PCE of P3HT/PCBM, reported to be over 5.5%,[13,14] is much lower than the theoretical limit, and a number of promising alternatives are currently being investigated.[15−19]

Organic solar cells are generally fabricated in a sandwich configuration, where a blend of donor and acceptor is placed between two electrodes, one of which is transparent. There are four main processes inside the solar cells controlling the PCE. The incoming light excites the polymer, forming mobile excitation (exciton) with an efficiency η_{EX}. The excitons migrate toward the interface between the donor and the acceptor where charge separation (CS) takes place: the electron localized in the LUMO of the donor is transferred to the LUMO of the acceptor to form a charge-transfer (CT) state. The electrons and holes will migrate to the electrodes under the influence of the electric field generated by the equalization of the Fermi energies of two electrodes where they will be collected (charge collection (CC)). It is also possible for the hole−electron pair to recombine, reducing the PCE through a charge recombination (CR) process. The total charge generation efficiency η_{tot} is affected by the efficiency of the component processes η_{EX}, η_{CS}, η_{CC}, and η_{CR}, and optimization of the solar cells can be seen as the simultaneous maximization of η_{EX}, η_{CS}, and η_{CC} and the minimization of η_{CR}. However, it is difficult to build a direct relation between every η component and the chemical structure of the interface, and for this reason, there are no simple design rules for organic photovoltaic materials besides the correct energy level alignment and the processability they should have. The preliminary step toward the design of organic photovoltaic materials is prediction of the rate of the elementary processes taking place within the cell. Some of these elementary processes (absorption, exciton, and charge migration) do not involve interfaces and can be studied in bulk materials.[20,21] The CS and CR are the two key interfacial processes whose competition influences more directly the PCE. Predicting the rate of these two processes is the first step to estimate the efficiency of charge generation at the interface and to guide the design of new materials.

Received: September 24, 2010
Revised: December 7, 2010
Published: January 10, 2011

The aim of this paper is to evaluate the absolute rates of CR and CS in an idealized model representing the P3HT/PCBM interface. It is assumed that the Marcus−Levich−Jortner (M−L−J)[22−24] expression of the rate constant is valid and all the parameters entering in the model will be computed with a variety of computational chemistry methods. This study will find the most suitable method for the P3HT/PCBM system and establish how accurately the different terms entering in the expression of the rate can be evaluated. We will see that while some of these terms can be evaluated accurately (internal reorganization energy), others have larger intrinsic inaccuracies (external reorganization energy and Gibbs free energy difference, electronic coupling), especially in the absence of a microscopic model of the interface. We will study the effect of these inaccuracies on CR and CS rates evaluation.

While the majority of the investigations on P3HT/PCBM solar cells has focused on the relation between the processing and the PCE,[3,6−13] fewer investigations have focused on the measurement of the elementary charge-transfer processes, providing the experimental data we wish to compare with. By using time-resolved terahertz spectroscopy, Ai and Beard[6] reported the photoinduced charge carrier generation dynamics of P3HT/PCBM blended films, finding that k_{CS} was faster than 4.0×10^{11} s^{-1} and k_{CR} was 2.5×10^{9} s^{-1} in the sample with the best photon-to-carrier yield. Kim and Fukuzumi[14] synthesized and characterized a BHJ solar cell made by a series of thienyl-substituted methanofullerenes as acceptors and P3HT as donor; they reported $k_{CS} = 5.0 \times 10^{11}$ s^{-1} and $k_{CR} = 3.1 \times 10^{8}$ s^{-1} for P3HT/PCBM, which had the highest PCE (4.2%) within the series. Piris and Siebbeles[25] studied the dynamics of charge carriers and excitons in thin films of P3HT/PCBM by using ultrafast optical pump−probe spectroscopy and reported the lower limit for k_{CS} as 5×10^{11} s^{-1}. Ohkita and Durrant[8] studied the charge carrier formation in polythiophene/fullerene blended films by transient absorption spectroscopy and found that a large LUMO level offset (free energy difference of charge separation process) will improve the charge dissociation efficiency. To sum up the experimentally available data, k_{CS} was reported to be faster than 4×10^{11} s^{-1} and k_{CR} was between 10^{8} and 10^{9} s^{-1}, certainly influenced by a variety of factors including the regioregularity of P3HT, solvent, film thickness, annealing temperature and time, and blended film composition.[26]

Computational models of organic bulk heterojunctions have been considered by several groups with different focuses. Kanai and Grossman[9] studied the electronic structure of the P3HT/C_{60} interface by density functional theory (DFT) calculation and looking mostly at the relative orbital energy alignment. Some key theoretical challenges of modeling charge photogeneration in organic solar cells have been discussed by Brédas and co-workers.[20] Brédas and Cornil studied the rates of charge separation and recombination of the phthalocyanine (donor)/perylene-tetracarboxylic-diimide (acceptor) solar cell in detail by using Marcus or M−L−J equations.[27,28] They also investigated the impact of the interface geometry on the CR and CS rates of pentacene/C_{60} and poly(*p*-phenylenevinylene)/C_{60} solar cells and found that the rates are strongly sensitive to the relative position of the donor and acceptor units; the performance of pentacene/C_{60} devices based on interfacial structure can suffer more from the CR process than devices based on bilayer heterojunctions.[20,29] However, there is little theoretical investigation on the absolute charge-transfer rate of elementary processes of P3HT/PCBM solar cells.

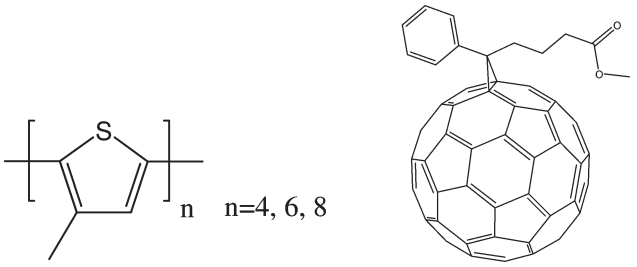

Figure 1. Chemical structures of $P3MT_n$ (n = 4, 6, and 8) and PCBM.

We begin our study in the next section by defining the molecular models used to describe the P3HT/PCBM interface and providing the computational methodology used in this work with the detail needed for evaluation of each parameter entering in the M−L−J equation. In the results section, k_{CR} and k_{CS} will be given and compared with the experimental values. One of the most challenging aspects of this calculation is that the rate depends on many parameters whose calculation, performed with different methods, is characterized by different degrees of accuracy. For this reason, we will discuss in detail the sensitivity of the computed rates on the input parameters and the relative accuracy of the computed rate.

2. METHODS

Models. To model the P3HT/PCBM interface, one PCBM molecule and one oligomer (regioregular) containing six thiophene rings were considered (Figure 1). The starting geometry for this reference structure is given in the Supporting Information (Figure S1). Kanai and Grossman[9] used four thiophene oligomers in a unit cell to study the electronic structure of C_{60} and P3HT. Moreover, the effective conjugation length of polythiophene was experimentally evaluated between 6 and 12 thiophene rings.[30] Thus, the smaller (4 thiophene rings) and larger (8 thiophene rings) donor model are also included in selected calculations for comparison. The hexyl groups on P3HT are replaced by methyl groups (P3MT is poly(3-methylthiophene)) because it has been confirmed that the side alkyl chain has hardly any effect on the electronic structure and optical properties of the polymer and is just used to increase the solubility.[31,32] Since the electronic coupling is expected to change with the different relative orientation,[28,29] we considered seven additional relative orientations of the P3MT/PCBM pair (8 orientations in total), whose detail is given in the Supporting Information (Figure S2 and Table S1). The properties other than the electronic coupling are computed with the orientation labeled as "8" in the Supporting Information.

Rate Expression. Considering that the electronic coupling between the donor and the acceptor is weak, we assume that the charge transfer between them can be described by the theory of nonadiabatic electron transfer. As we will see, the nuclear relaxation following the electron transfer involves mostly intramolecular (high-frequency) modes, and so we chose the M−L−J equation[22−24] formulation of the rate expression which, unlike the simpler Marcus equation, includes the effect of the quantum vibrational modes in an effective way

$$k_{et} = \frac{2\pi}{\hbar}|V|^2 \frac{1}{\sqrt{4\pi\lambda_{ext}K_B T}} \sum_{\nu} \exp(-S^{eff}) \frac{(S^{eff})^{\nu}}{\nu!} \exp\left(-\frac{(\lambda_{ext}+\nu\hbar\omega^{eff}+\Delta G)^2}{4\lambda_{ext}K_B T}\right) \quad (1)$$

dx.doi.org/10.1021/jp109130y |J. Phys. Chem. C 2011, 115, 2406–2415

where V is the electronic coupling between the initial and the final states, λ_{ext} is the external reorganization energy, S^{eff} is the effective Huang−Rhys factor, ω^{eff} is the frequency of one effective mode that incorporates in an average way the effect of all quantum modes, ΔG is the Gibbs free energy difference between the initial and the final states, T is the temperature, K_B is the Boltzmann constant, and $\hbar$ is the reduced Planck constant. The summation of ν runs over all possible vibrational modes. The following sections will describe how to compute $\Delta G_{CS}/\Delta G_{CR}$, λ_{ext}, V_{CS}/V_{CR}, S^{eff}, and ω^{eff}, providing a more detailed definition of these quantities when appropriate.

Charge-Transfer State Energy and Gibbs Free Energy Difference. Full geometry optimization of the isolated neutral ($P3MT_n$ and PCBM) and charged ($P3MT_n^+$ and $PCBM^-$) molecules were performed at the DFT[33,34] level with Becke's three-parameter functional and the Lee−Yang−Parr functional (B3LYP)[35] level associated with the 6-31G* basis set. There is considerable discussion in the literature concerning the development of appropriate density functionals to study charge-transfer states as it is known that some charge-transfer states are occasionally poorly described by the standard density functional because of the long-range self-interaction error.[36−39] As we will see, B3LYP provides a reasonable description of the states we are interested in, but, to highlight the possible role of the density functional in our results, we will also present selected single-point calculations with hybrid functionals mPW1PW91[40] and M06-HF[36] which implements an improved long-range behavior.

The charge-transfer state is essentially an excited state of a very large molecular complex, and for this reason, its electronic structure and energy are not easy to evaluate accurately. In a recent investigation carried out by Cornil,[28] the energies of the neutral donor and acceptor (E^D and E^A) and the energies of the charged donor and acceptor (E^{D+} and E^{A-}) were computed for the isolated species as well as the energy of the isolated excited donor (E^{D^*}). ΔG_{CR} and ΔG_{CS} were calculated by $E^D + E^A - E^{D+} - E^{A-} + \Delta E_{coul}$ and $E^{D+} + E^{A-} - E^{D^*} - E^A + \Delta E_{coul}$, respectively, where ΔE_{coul} is the Coulombic interaction between the donor and the acceptor. This approximation is valid if the main interaction term between the donor and the acceptor is the Coulombic one. However, these molecules are very close and very polarizable, and so it is very likely that the vicinity of the donor−acceptor pair modifies their electronic structure. We attempt here a more accurate calculation of the Gibbs free energy difference (CR and CS) by including the donor and acceptor in a single and larger computational model.

The Gibbs free energy difference of the charge recombination (ΔG_{CR}) and separation (ΔG_{CS}) processes was calculated as follows

$$\Delta G_{CR} = E_{P3MT^0/PCBM^0} - E_{CT} \quad (2)$$

$$\Delta G_{CS} = E_{CT} - E_{P3MT^*/PCBM^0} \quad (3)$$

where $E_{P3MT^0/PCBM^0}$ and $E_{P3MT^*/PCBM^0}$ are the energy of the neutral molecule model before and after excitation of P3MT calculated by the isolated P3MT and PCBM molecules. The energy difference between the $P3MT^0/PCBM^0$ dimer energy and the sum of the energy of the isolated molecules is very small (0.02 eV) because the Coulombic interaction is small. It is therefore reasonable to assume that $E_{P3MT^*/PCBM^0}$ can also be represented by the sum of the isolated molecular component in $E_{P3MT^*} + E_{PCBM^0}$ (E_{P3MT^*} is calculated by the TDDFT method) within a small error. However, we cannot simply use $E_{P3MT^+} + E_{PCBM^-}$ to represent E_{CT} because the interaction between the charged fragments, $P3MT^+$ and $PCBM^-$, is large. To better evaluate the error intrinsic in the calculation of the charge-transfer state energy, three methods were used to describe this state.

(i) TDDFT[33,34] is the most extensively used method to study the excited states of medium-sized molecules.[41] Here, it is used to compute the vertical singlet (and triplet) excited states from the ground state in its equilibrium geometry. The first excited state should correspond to the configuration where an electron is excited from the polymer HOMO to fullerene LUMO, representing the CT state. However, the TDDFT energy of the CT state computed in the geometry of the ground state is not exactly equal to the energy in the potential energy minimum of the CT state required for the calculation of ΔG_{CR} and ΔG_{CS}.

(ii) Unrestricted DFT (UDFT) was used to optimize the lowest-lying triplet excited-state geometry of P3MT/PCBM.[42] If two unpaired electrons in the singly occupied molecular orbitals are localized on P3MT and PCBM, respectively, then we can use this lowest-lying triplet excited state to approximate the geometry and energy of the CT state. It is, in fact, difficult to optimize the geometry of the singlet excited state for such a large system (TDDFT excited-state optimizations are computationally expensive), but we found that the lowest singlet and the triplet excitation energies are almost the same by the TDDFT method (see below) because the unpaired electrons are well separated and the exchange interaction is negligible. These calculations have been performed with the B3LYP functional, but similar results were obtained with the mW1PW91[40] functional with improved long-range behavior.

(iii) The interaction between $P3MT^+$ and $PCBM^-$ in a charge-transfer state can be considered by performing the calculation of one component of the pair in the presence of *background charges* (BC), reproducing the electrostatic potential of the second component of the pair. This will include their Coulombic and polarization interaction.[43] First, the charges of $P3MT^+$ ($PCBM^-$) fitting to the electrostatic potential at points were calculated according to the CHelp[44] scheme based on the optimized geometry of $P3MT^+$ ($PCBM^-$). Then, the energy (E_{BC}) of $PCBM^-$ ($P3MT^+$) was calculated in the presence of the BC of $P3MT^+$ ($PCBM^-$). Using also the result of the energy calculation without BC, the electrostatic interaction energy between the pair can be computed as $E_I = 1/2[E_{BC}(PCBM^-) - E(PCBM^-) + E_{BC}(P3MT^+) - E(P3MT^+)]$. Finally, E_{CT} can be calculated by $E_{BC}(PCBM^-) + E_{BC}(P3MT^+) - E_I$ (if E_I is not subtracted, the electrostatic interaction would be counted twice).

Internal Reorganization Energy. The reorganization energy of a charge-transfer reaction leading from a neutral to a charge-transfer state is defined as[45]

$$\lambda = \frac{1}{2}(E_0' - E_0 + E_{CT}' - E_{CT}) \quad (4)$$

where $E_{0/CT}$ is the energy of the neutral (CT) state computed in the equilibrium geometry of the neutral (CT) system and $E'_{0/CT}$ is the energy of the neutral (CT) state computed in the equilibrium geometry of the CT (neutral) state. λ is normally separated into the internal (or intramolecular, λ_{int}) and external (λ_{ext}) reorganization energy ($\lambda = \lambda_{int} + \lambda_{ext}$). The internal component of the reorganization energy can be obtained by an

explicit evaluation of the four energies in eq 4 for the model P3MT/PCBM system.[45]

λ_{int} is normally further decomposed into contributions along the various normal frequency modes i of the molecule according to[24,45]

$$\lambda_{int} = \sum_i S_i \hbar\omega_i \quad (5)$$

S_i is the Huang−Rhys factor of the corresponding frequency mode (with frequency ω_i); the summation of i runs over all vibronic modes. The analysis of the electron transfer rate is greatly simplified by defining effective frequency ω^{eff} and effective Huang−Rhys factor $S^{eff} = \sum_i S_i \hbar\omega_i/\omega^{eff}$, so that it is possible to consider a single effective degree of freedom for the reaction coordinate (S^{eff} and ω^{eff} appear in eq 1). It is straightforward but generally unnecessary to consider explicitly more modes.[22]

External Reorganization Energy. The external reorganization energy is the contribution to eq 4 due to the reorientation of the surrounding molecules in the charge-transfer process. λ_{ext} is much smaller in the solid phase than in liquids, but it still accounts for a good fraction of the total reorganization energy when the charge transfer involves molecules with small λ_{ext} as in this case. Several authors leave λ_{ext} as an adjustable parameter or use an order of magnitude estimate.[46,47] For smaller molecules in the condensed phase it is possible to use a QM/MM[48] or a polarizable force field[49] to perform a direct evaluation, but in the absence of detailed structural information on the interface, one has to resort to classical dielectric continuum models[50] as done, for example, by Cornil[28,51] et al. Following the latter approach, we calculated λ_{ext} as[52−54]

$$\lambda_{ext} = \frac{1}{4\pi\varepsilon_0}\Delta e^2\left(\frac{1}{2a_1}+\frac{1}{2a_2}-\frac{1}{R}\right)\left(\frac{1}{\varepsilon_{OP}}-\frac{1}{\varepsilon_0}\right) \quad (6)$$

where a_1, a_2, R, ε_{OP}, and ε_0 are donor radii, acceptor radii, the distance between the centers of the donor and acceptor, and optical and zero-frequency dielectric constants of the surrounding media, respectively. Moreover, ε_{OP} can be calculated by $\varepsilon_{OP} = n^2$ (n is the refractive index of P3HT/PCBM). λ_{ext} is computed with much less accuracy than the other terms appearing in eq 1, first because of the intrinsic approximations of the continuum model and then because of the uncertainty in the measurement of ε_{OP} and ε_0 caused by the different conditions and experimental setup. Thus, the range of λ_{ext} that can be computed from a range of plausible parameters entering eq 6 is rather large, and its effect on the computed rate is discussed more in detail below. The equation is strictly valid for spherical molecules, and the approximation needed to define the effective radii a_1 and a_2 further reduce the accuracy of this estimate. The experimental uncertainty on the dielectric constant will affect in a similar way the evaluation of the λ_{ext} based on the continuum model even if more complicated models[55,56] are adopted or the Poisson−Boltzmann equation is solved.[57] QM/MM methods[48] would offer an ideal solution to improve the accuracy of λ_{ext}, but they can be used only if an atomistic model of the interface is available and the polarizability of the molecular fragments can be validated through experiments, two conditions that are not satisfied in our case.

Electronic Coupling. As the P3MT excited state is dominated by the HOMO → LUMO transition (the corresponding configuration makes up more than 80% of the excited-state wave function), the electronic coupling in the charge separation process (V_{CS}) is taken to be the coupling between the LUMO of P3MT and PCBM. In PCBM, the LUMO + 1 is energetically very close to the LUMO and the charge-transfer state corresponding to the electron transfer between P3MT LUMO and PCBM LUMO + 1 is only 0.04 eV higher in energy than the lowest energy charge-transfer state. For this reason we also compute the electronic coupling between P3MT LUMO and PCBM LUMO + 1. The electronic coupling in the charge recombination process (V_{CR}) is taken to be the coupling between the HOMO of donor and the LUMO or LUMO + 1 of the acceptor. The electronic coupling V_{ij} between the orbitals ϕ_i and ϕ_j of the isolated fragments is defined as $\langle\phi_j|\hat{F}^0|\phi_i\rangle$, where $\hat{F}^0$ is the Kohn−Sham−Fock operator of the total system evaluated by assuming the density matrix of the isolated fragments.[58]

Alternative methods for calculation of the electronic coupling have been proposed in recent years including, for example, energy level splitting,[59] generalized Mulliken−Hush,[60] fragment charge difference,[61] and constrained DFT,[61] and a number of papers have proposed comparison of coupling calculation with level of theory,[62,63] basis set,[64] and methods.[65] Considering the variations observed in these studies (see, for example, ref 62), we can consider our evaluated calculation of the coupling, at a fixed configuration, correct within a factor of ∼1.5.

All of the quantum chemical calculations of this paper were completed by Gaussian 03.[66]

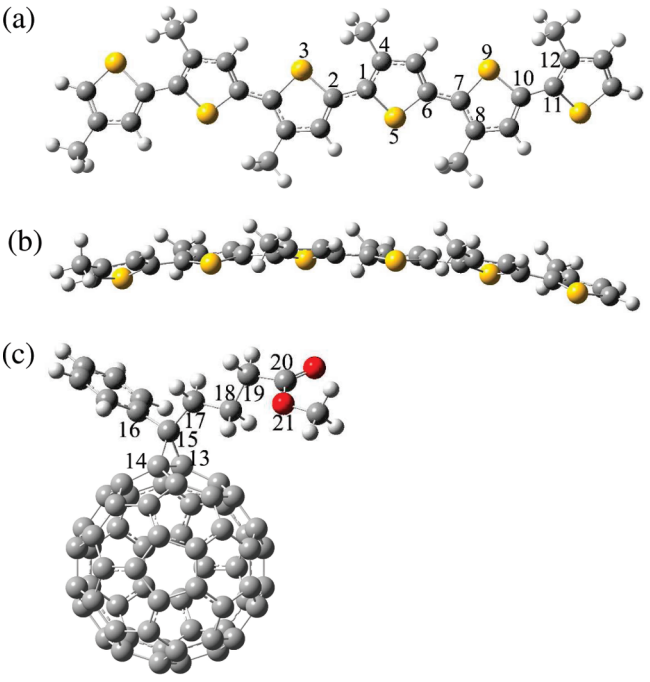

Figure 2. Optimized geometry of the neutral P3MT$_6$ (top (a) and side (b) views) and PCBM (c).

3. RESULTS AND DISCUSSION

Geometries of the Isolated P3MT and PCBM. We found that the neutral optimized geometry of P3MT$_n$ and PCBM are consistent with the previous experimental and theoretical results of oligomers[67−71] and the geometry of P3MT$_n$ is similar for n = 4, 6, and 8 (P3MT$_6$ and PCBM are shown in Figure 2). The geometry of PCBM is not changed much from the neutral to

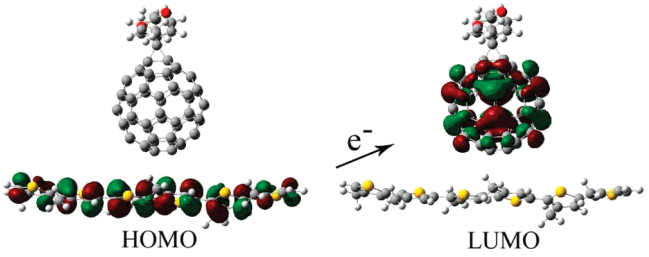

Figure 3. Frontier orbitals of $P3MT_6$/PCBM involved in the singlet and triplet excitation processes obtained by the TDDFT method (optimized ground-state geometry).

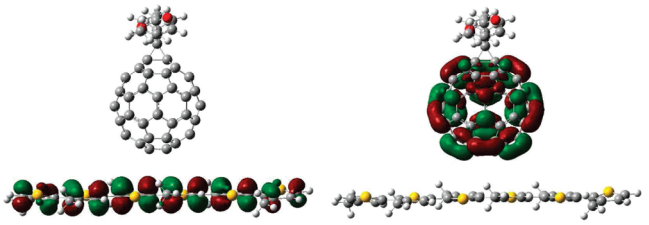

Figure 4. Singly occupied molecular orbitals in the lowest triplet state of the $P3MT_6$/PCBM model obtained by the UDFT method (optimized excited-state geometry).

charged molecule, and the only important structural change involves the P3MT molecule. The structure of $P3MT^+$ is nearly planar, with the dihedral angles S3−C2−C1−C4, S5−C6−C7−C8, and S9−C10−C11−C12 being close to 0.0°, which is different from the structure of the neutral molecule where the same angles take values between 14.7° and 23.1°.

Excitation Energy of P3MT. The first singlet excitation process of $P3MT_n$ (n = 4, 6, and 8) is studied by the TDDFT method. The electron is excited from π to π^* on the whole chain of P3MT. Our calculated excitation energies of $P3MT_n$ (n = 4, 6, and 8) are 2.96, 2.49, and 2.25 eV, respectively, which are in agreement with the experimental excitation energies of oligomer $P3MT_n$ (n = 4 (3.16 eV), n = 6 (2.85 eV))[72] and other theoretical results (n = 4 (3.00 eV), n = 6 (2.45 eV), and n = 8 (2.35)).[73,74] The experimental absorption maximum in crystalline P3HT (∼2.0 eV) is a bit lower than the experimental value for the octamer, suggesting that, in the crystalline phase, P3HT may have a conjugation length longer than eight monomers and/or there is a significant $\pi-\pi$ stacking effect (which cannot be taken into account by our model).

Charge-Transfer State and Gibbs Free Energy Difference $\Delta G_{CS}/\Delta G_{CR}$. The isolated polymer and fullerene were put together to simulate the interface; the optimized separation distance between $P3MT_6$ and PCBM is about 3.7 Å (the starting separation distance is 3.5 Å, shown in Figure S1, Supporting Information), which is consistent with the typical value of 3.5 Å.[9] By using the TDDFT method, we studied the singlet and triplet excited-state properties of $P3MT_6$/PCBM. Both the first singlet and the lowest triplet excitation correspond to the configuration where the electron is excited from the HOMO localized on $P3MT_6$ to the LUMO localized on PCBM (the orbitals are shown in Figure 3). Since this is a charge-transfer configuration, with large separation between the unpaired electrons, the singlet (1.261 eV) and triplet (1.260 eV) excitation energies are essentially identical because of the negligible exchange interaction (after the triplet-state geometry relaxation, the singlet and triplet excitation energies are also nearly the same). A similar excitation energy (1.34 eV) is obtained using the hybrid functional mPW1PW91[40] including the improved long-range behavior, suggesting that these corrections are not as important for the current system. We should mention, however, that the choice of functional remains one of the crucial, still unsolved, problems for the computational study of photovoltaic systems. For example, an attempt to optimize the CT state with the M06-HF functional,[36] especially designed for charge-transfer states, led to unphysical results (i.e., chemical bonding between P3MT and PCBM).

It has been proposed and proved for some donor−acceptor pairs that the formation of a low-energy triplet state localized on the donor can be a possible loss mechanism.[75−77] In our model, however, the lowest energy triplet excited state of the donor is about 0.23 eV higher in energy than the charge-transfer state; so, within our small model, we can exclude formation of a triplet on P3MT as a possible loss mechanism. This may explain the very high quantum efficiency for charge separation observed in this system.[25]

For this reason we can optimize the lowest triplet excited-state geometry with a relatively cheap UDFT method instead of the much more expensive alternative CASSCF methods and assume that the geometry and energy of the triplet state are the same as the singlet charge-transfer state. We verified that spin contamination,[63,78] which is a major source of error in unrestricted calculations, is rather small in this case: the expectation value of the squared spin angular momentum, $\langle S^2 \rangle$, is less than 2.01 for the triplet state. The calculated frontier orbitals of $P3MT_6$/PCBM obtained by the UDFT method and the UDFT-optimized geometry are shown in Figure 4. In the $P3MT_6^+$/$PCBM^-$ pair in the triplet equilibrium configuration, the four central thiophene rings tend to stay planar (the dihedral angles S3−C2−C1−C4 and S5−C6−C7−C8 are less than 5.0°), while the terminal thiophene rings deviate from planarity (the dihedral angle S9−C10−C11−C12 is 15.2°), in contrast with what is observed with the isolated $P3MT_6^+$, which is wholly planar. This is clearly an effect of the neighboring highly polarizable $PCBM^-$, which stabilizes more the positive charge on the center of the oligomer chain. The C1−C2 bond in the charged polymer is shortened by about 0.01 Å, but the C−C and C═C bonds in PCBM are hardly changed. Figure 4 shows that the frontier orbitals obtained by UDFT are similar to those obtained by the TDDFT method (Figure 3), i.e., the nature of these orbitals is not modified by the nuclear deformation following the charge transfer. The hybrid functional mPW1PW91 (with improved long-range behavior) is also used to optimize the geometry of the triplet state, which gives similar triplet charge-transfer state properties and energy (1.59 eV) as B3LYP (1.52 eV) relative to the ground state. Thus, UDFT can be used to describe the properties of the charge-transfer state.

The calculated $P3MT_4$/PCBM and $P3MT_6$/PCBM frontier orbitals are similar. In contrast, both of the singly occupied orbitals of the $P3MT_8$/PCBM triplet are localized on the polymer (these orbitals are illustrated in the Supporting Information), i.e., the two unpaired electrons cannot be separated in the lowest triplet excited states because the LUMO energy of P3MT is lower than that of PCBM on increasing the number of thiophenes from 6 ($P3MT_6$) to 8 ($P3MT_8$). In other words, the $P3MT_8$/PCBM model has the wrong qualitative structure of the energy levels to be able to describe the realistic P3HT/PCBM interface. This could be due to a number of limitations of DFT or the lack of dielectric screening in our model, the investigation of which is outside the scope of this work.

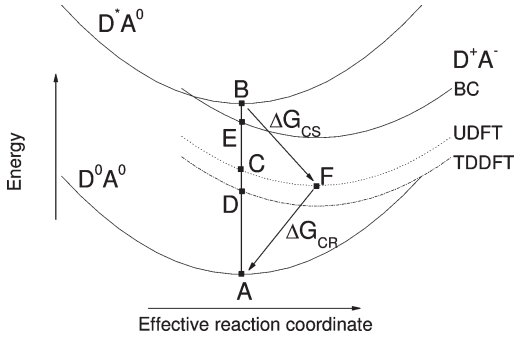

Figure 5. Schematic diagram of the potential energy curves appropriate for the states of interest and the energy points that have actually been evaluated.

Table 1. Energy (in eV) of the Key Points in the Potential Energy Surface (Figure 5) Relative to the Ground-State Energy E_A

	P3MT$_4$/PCBM	P3MT$_6$/PCBM	calcd	expt
E_B	2.96	2.49		
E_C	1.77	1.76		
E_D	1.44	1.24		
E_E	2.26	2.11		
$-\Delta G_{CR} = E_F$	1.64	1.52	1.4[80]	1.1[8,81]
$-\Delta G_{CS} = E_B - E_F$	1.32	0.97		0.9[8,81]

Unlike TDDFT and UDFT, the BC method can always be used to describe the charge-transfer state properties because the system is forced into the charge-transferred configuration.

Figure 5 provides a scheme of the potential energy surface of the system with the energy points indicated with letters A−F computed by various methods. E_A is the equilibrium ground-state energy computed with the DFT method; E_B is the vertical energy of the excited state caused by light absorption in the same geometry of the ground state (nuclear relaxation of the excited state is neglected) computed with TDDFT. E_C, E_D, and E_E are the vertical excitation energies computed with TDDFT, UDFT, and BC methods, respectively. The energy in the optimized geometry of the triplet excited state by UDFT is E_F. Table 1 shows the energy of points B−F relative to the energy of point A.

Table 1 shows that ΔG_{CR} and ΔG_{CS} of P3MT$_6$/PCBM calculated by the UDFT method are −1.52 and −0.97 eV, respectively. E_E is about 0.35 and 0.87 higher than E_C and E_D, respectively. It has been confirmed that the driving force of the charge separation should be much larger than 0.3 eV to ensure the effective charge separation process,[79] so the results obtained by the BC method are not acceptable. The CT state energies obtained by TDDFT and UDFT are relatively close to one another and reasonable; however, only UDFT can give, at an acceptable computational cost, the required equilibrium geometry and energy needed to compute ΔG_{CR} and ΔG_{CS}, and these computed values are the ones carried forward for evaluation of the rate. ΔG_{CR} of P3MT$_4$/PCBM is close to that of P3MT$_6$/PCBM, while ΔG_{CS} of P3MT$_4$/PCBM is more negative than that of P3MT$_6$/PCBM, which is the result of the large excitation energy of P3MT$_4$ due to the shorter conjugation length. Considering the poor value of ΔG_{CS} in comparison with the experimental estimates (also given in Table 1) we conclude that also P3MT$_4$/PCBM is not suitable for modeling of the P3HT/PCBM interface.

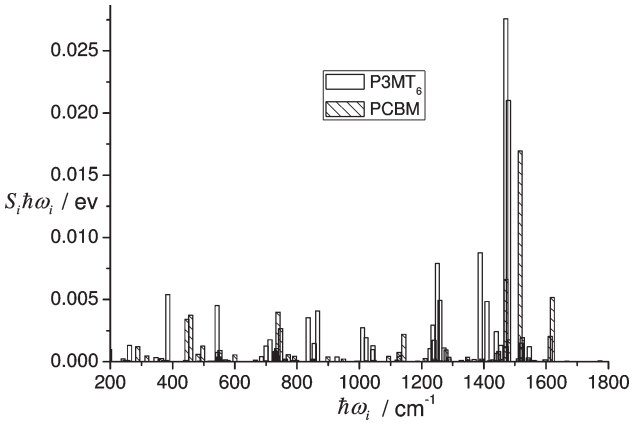

Figure 6. Plot of the distribution of the $S_i\hbar\omega_i$ over the different vibronic modes $\hbar\omega_i$ of P3MT$_6$/PCBM.

Experimentally, the energy of the charge-transfer state E_{CT} is estimated from a simplified version of the Weller equation[82] $E_{CT} = IP_{polymer} - EA_{fullerene}$ (IP is the ionization potential and EA is the electron affinity). Experimentally, IP_{P3HT} and EA_{PCBM} are reported to be 4.8 and 3.7 eV, respectively.[8,81] Therefore, the energy of the charge-transfer state is estimated to be 1.1 eV higher than the energy of the ground state. The excitation energy was ∼2.0 eV for the crystalline polymers by absorption and PL spectra.[8] Thus, ΔG_{CS} is around −0.9 eV. An alterative theoretical evaluation based on DFT calculation gives for ΔG_{CS} a value of −1.4 eV by Van Voorhis,[80] which is consistent with ours (−1.52 eV).

Evaluation of the Internal and External Reorganization Energy. The total internal reorganization energy is 0.250 eV when the donor and acceptor are treated separately and 0.254 eV when the donor and acceptor are considered together in a single calculation, and these values are very similar to the 0.27 eV value obtained by Vandewal by fitting of the charge-transfer band in the photovoltaic external quantum efficiency.[83] To evaluate how the internal reorganization energy is distributed along the various normal modes of the molecule, we computed the individual components of the reorganization energy (see eq 5). Figure 6, showing $S_i\hbar\omega_i$ versus the corresponding frequency $\hbar\omega_i$, shows that the C═C (1400−1600 cm^{-1}/0.17−0.2 eV) bond stretchings are the main and strongest vibrational modes contributing to the λ_{int}, so we set the effective frequency ω^{eff} to be 1500 cm^{-1} (0.186 eV) and the corresponding S^{eff} is 1.366. The effect on the computed rates of changing the parameter ω^{eff} within a reasonable range is discussed below.

The effective radius of P3MT$_6$ and PCBM molecules, needed for evaluation of λ_{ext} from eq 6, are calculated as the radius of the molecule sphere volume defined as the volume inside a contour of 0.001 electrons/bohr^3 density.[84,85] The distance between the mass centers of the P3MT$_6$ and PCBM is 9.0 Å. The dielectric constant ε_0 of P3HT/PCBM is measured to be 3.4 and 3.8 by Koster et al. and Glatthaar et al., respectively, intermediate between that of P3HT (3.0) and PCBM (3.9).[86,87] The refractive index of polythiphene and P3HT/PCBM is measured to be 1.4 and 1.6 by using excitation wavelengths of 633 and 450 nm by Hoppe,[88] Moulé,[89] and Hillman.[90] Therefore, the optical frequency dielectric constant (ε_{OP}) of polythiophene and P3HT/PCBM is 1.96 and 2.56. The calculated external reorganization energy of P3MT$_6$/PCBM according to various ε_{OP} and ε_0 are in the range of 0.06−0.18 eV, which is somewhat broader than

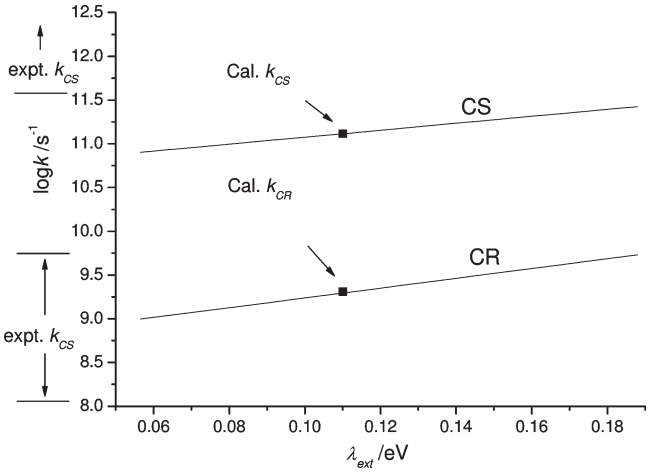

Figure 7. Evolution of k_{CS} and k_{CR} as a function of the external reorganization energy, λ_{ext}, of P3MT$_6$/PCBM, together with the experimental rate range, V_{CR}/V_{CS} = 13.0/13.6 meV, $\Delta G_{CR}/\Delta G_{CS}$ = −1.516/−0.969 eV, S = 1.366, $\hbar\omega$ = 0.186 eV.

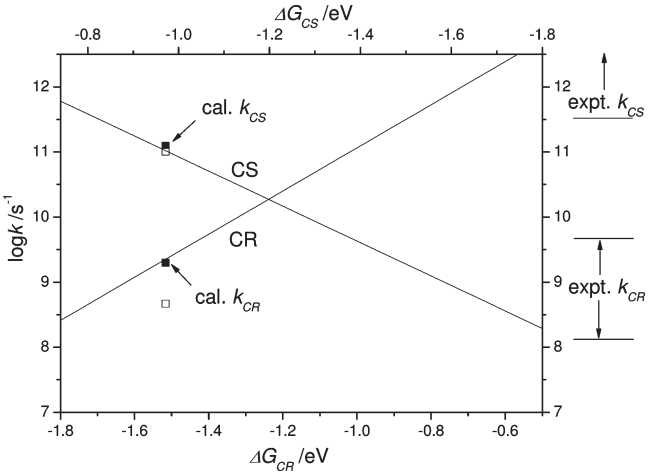

Figure 8. Evolution of k_{CS}/k_{CR} as a function of the Gibbs free energy difference $\Delta G_{CS}/\Delta G_{CR}$ of P3MT$_6$/PCBM, together with the experimental rate range. V_{CR}/V_{CS} = 13.0/13.6 meV, λ_{ext} = 0.11 eV, S = 1.37, $\hbar\omega$ = 0.186 eV (■), S = 1.71, $\hbar\omega$ = 0.149 eV (□).

desirable. For this reason we will evaluate the rate for a range of external reorganization energies and use 0.11 eV as the average reference value.

Evaluation of the Electronic Coupling. For the calculation of the rate we use the appropriate electronic coupling averaged over the different considered orientations. The squared average of n different values of coupling V is defined as $(\sum_i V_i^2/n)^{1/2}$, and the individual values are given in the Supporting Information (Table S2). The average V_{CS} and V_{CR} are 8.7 and 8.5 meV, respectively, if the LUMO of PCBM is considered the only orbital on the acceptor. If we assume that also the LUMO + 1 orbital can accept an electron the average couplings are slightly modified to 13.0 and 13.6 meV, respectively, and the latter values are used in the rate calculation below.

Rate of Charge Separation (k_{CS}) and Recombination (k_{CR}). The parameters computed above can be readily substituted in eq 1 to obtain the desired charge separation and recombination rates (k_{CS} and k_{CR}). More than the value itself, it is more instructive to compute how these rates depend on the parameters that are more difficult to evaluate. We compared the computed rate with the range of experimentally available rates described in the Introduction. We started considering the dependence of k_{CS} and k_{CR} on λ_{ext}, the parameter with the largest relative uncertainty. Figure 7 shows that our calculated k_{CS} varies by about 1 order of magnitude as λ_{ext} is varied within the acceptable range, and a similar variation is observed for k_{CR}. Although it would be desirable to have a better evaluation of λ_{ext}, its accurate determination seems not to play such a key role in the prediction of relative reaction rates once the appropriate range has been determined. To analyze the effect of other parameters on the computed rates we set the external reorganization energy to the average value λ_{ext} = 0.11 eV in the continuation of this analysis (leading to k_{CS} =1.51 × 10^{11} s^{-1} and k_{CR} = 1.93 × 10^9 s^{-1}).

Although we have a relatively robust evaluation of the energy of the charge-transfer state, this remains one of the most challenging parameters to be computed. For this reason we presented the variation of k_{CS} and k_{CR} as a function of ΔG_{CS} and ΔG_{CR} (ΔG_{CS} + ΔG_{CR} is kept constant, assuming that the excitation energy is constant) in Figure 8. Here, the variation of the computed rates with the energy location of the CT state is more dramatic. One order of magnitude change in the rate is computed if the energy of the CT state is under- or overestimated by 0.2 eV, and our different attempts to evaluate the CT state indicate that inaccuracies of ∼0.2 eV or larger are indeed possible for systems of this size. The k_{CR} computed with the ΔG_{CR} given in Table 1 is well within the experimental range, while k_{CS} computed with the same parameters set are little lower than the experimental values.

Finally, we also consider the effect of the choice of the effective frequency ω^{eff} on the computed rates. As Figure 6 shows that there is hardly any contribution to λ_{int} from frequencies higher than 1700 cm^{-1}, we recomputed the rates using the smaller value ω^{eff} = 1200 cm^{-1}, about 20% smaller than the one used up to this point. This change causes a reduction of k_{CS} to 1.09 × 10^{11} s^{-1} and of k_{CR} to 4.86 × 10^8 s^{-1} (also shown in Figure 8). While these variations, in particular on k_{CR}, may be considered significant they are not a cause of concern. It is, in fact, always possible to drop the approximation of having a single effective mode and perform the calculation with more modes (or, in principle, with all modes).[22]

Figures 7 and 8 show that the computed k_{CR} overlaps with the range of experimentally determined rates while the computed k_{CS} is a little bit lower compared to the experimental range. It appears that a less negative ΔG_{CS} value would perfectly align the computed rates with the experimental one. There are two easily identifiable reasons that would make ΔG_{CS} less negative. First, it is possible that the electron is transferred to a highly excited CT state corresponding to excitation from the HOMO of the polymer to the LUMO + 1 or LUMO + 2 of the PCBM. The energy of these states (estimated from TDDFT calculations of T_2 and T_3) are 0.047 and 0.202 eV higher than the lowest energy charge-transfer state. Another important effect that may make ΔG_{CS} less negative is the electron transfer into a partially delocalized orbital comprising several PCBM molecules. It was in fact shown, at least far from the interface, that the morphology of both PCBM and P3HT generates a complicated distribution of partially localized states.[91,92] It may therefore be necessary to consider the charge-transfer reaction between states close to the interface not necessarily made, for example, by a single PCBM

molecule but by a cluster of molecules. It is not easy to compute the effect of partial electron delocalization on ΔG_{CS}, but an estimate can be attempted based on simple electrostatic and scaling arguments. Indicating with $\Delta G_{CS}(1)$ as the value appropriate in the case of a single PCBM acceptor, in the case of N PCBM molecules acting as electron acceptors the corresponding $\Delta G_{CS}(N)$ is less negative because the negative charge is more separated from the positive charge in the polymer. A rough estimate of $\Delta G_{CS}(N)$ can be given by

$$\Delta G_{CS}(N) \approx \Delta G_{CS}(1) - \frac{e^2}{4\pi\varepsilon_0}\left(\frac{1}{a_1 + a_2 N^{1/3}} - \frac{1}{a_1 + a_2}\right) \quad (7)$$

which causes, for example, an increase of ΔG_{CS} by about 0.31 eV when N is 5, placing the computed rate within the experimental range.

Another interesting experimental observation to compare with is that the charge separation process is virtually temperature independent with an activation energy on the order of few meV. Our rate expression in eq 1 is more complicated than an Arrhenius-like rate, but the activation energy can be defined anyway as $E_a = -K_B d \log k_{CS}/d(1/T)$. Using this definition we obtained E_a = 4.7 meV (at T = 300 K with $\Delta G_{CS} = -0.97$), encouragingly close to the experimental value.[93]

In this work we neglected the emergence of interface dipoles at the donor/acceptor interface of the device, as this effect can only be studied from first principles with a model of a 2D interface, not a simple donor−acceptor pair.[94] The accurate calculation electrostatic potential and the energy level bending at this interface is essential for the process of complete charge separation of the change transfer state initially formed at the interface.[95] Experimentally, the interfacial dipole E_{DIP} in controlled interfaces between P3HT and C_{60} is about 0.6 eV (charge is transferred from the polymer to the C_{60}). The effect of these dipoles on the rate that we compute depends on the nature of the charged interface for which there is not a unique interpretation. If one assumes that the interface dipole is due to dipolar/quadrupolar potentials of the component materials[95] or it can be described by an induced density of states model,[96] the potential energy drop across the interface will be distributed within 1−2 molecular layers resulting in an increase of the CT state energy of several tenths of eV. From Figure 8, one can evaluate how this will cause a decrease of k_{CR} and an increase of k_{CS}. However, Braun et al. suggest, on the basis of spectroscopic evidence, that the interface potential emerges from the transfer of integer charge between few molecules.[94] To justify a 0.6 eV interface dipole across a ∼1 nm interface one has to assume a charge density of 5.3×10^3 C/m^2 corresponding to one electronic charge every 3000 nm^2. Therefore, if integer charge is transferred between (few) donor and acceptor molecules the electrostatic at the interface will be very inhomogeneous with the majority of the donor−acceptor pairs being far from a strong electric field and few pairs in contact with charge-separated species. This situation may lead to a broader distribution of rates which can be again deducted from Figure 8.

4. CONCLUSION

In this work we have shown that it is possible to use a simplified model system to study the rates of interfacial charge separation and recombination in the prototypical bulk heterojunction organic solar cell based on the P3HT/PCBM blend. We were able to obtain rates comparable with those observed experimentally by using a model of the polymer containing only six oligomers and a single PCBM molecule. To compute the rate we assumed the validity of the M−L−J approach and used a variety of methods to calculate all the ingredients required for evaluation of the rates. Some of these ingredients are simply obtained from methodologies extensively adopted and reviewed in the literature, e.g., the internal reorganization energy. Some others are less trivial to compute and can cause big uncertainties in the final computed rate. One of the difficult parameters to compute is the external reorganization energy, which we estimated using a simple continuum model. We found, however, that setting this value within the physically plausible range would modify the rate only by 1 order of magnitude, which, given the complexity of the problem, is not to be considered a very large error. The parameter that most influences the rate is the equilibrium energy of the charge-transfer state, which is also difficult to investigate experimentally. We proposed in this paper that a very efficient way to study the charge-transfer state is by considering the charge-separated triplet state instead of the singlet. TDDFT calculations show that this state is energetically identical to the singlet (as chemical intuition suggests), and it is expected to have the same geometry. The triplet charge-transfer state, however, can be very easily optimized via UDFT because it can be described by a single configuration and is the `ground state' of the manifold of triplet states. The situation is complicated in general by possible spin contamination effects (not present in our case) in the UDFT calculation and the erratic behavior of current density functionals when they are applied to the study of charge-transfer states.[36,63,97,98] We also considered evaluating the CT state via a background charges method, but the results were unsatisfactory when compared with the experimentally available data, probably because the method forces a too strong separation between the orbital wave function on the two fragments.

In presenting these results we stressed the sensitivity of the rate on the less accurate parameters that can be determined from first principles. Although the degree of agreement with the range of available experimental rates is very satisfactory, it is important to point out a few key improvements required to make the modeling of organic bulk heterojunctions of direct use to the experimental community. First, it is to be expected that the contact between PCBM and P3HT will not be identical across the interface, and it is therefore expected that the intermolecular coupling is different from site to site, and for this reason we used the average electronic coupling based on several different orientations of donor and acceptor. However, a more accurate modeling of this effect requires a MD/QC approach[29,99−103] (using molecular dynamic snapshots for quantum chemistry single point calculations), which is currently under development by our group for this particular system. Additional complications that may be considered in future work include the charge separation into more delocalized states or into highly excited electronic CT states. Finally, the competition between charge separation and charge recombination is crucial for the efficiency of the cell, but after a long-lived charge-transfer state is formed, another step not studied here involves migration of the hole and electron away from the interface. How the hole−electron pair can break, overcoming its Coulombic attraction, is not clear, and this step also needs to be modeled if one hopes to contribute to photovoltaic research through computational chemistry methods. It is also possible that the hole and electrons are directly dissociated at the interface without forming a bound pair.[80]

When computational chemistry is applied to photovoltaic research it can offer a reductionist view of the device operation, with elementary processes studied in isolation from all the other processes taking place in the cell. While we are far from being able to describe all the relevant processes in a fully consistent way, this paper has shown that the elementary charge separation and recombination steps at the interface can be described encouragingly well.

■ ASSOCIATED CONTENT

Supporting Information. Starting geometry of No. 8 P3MT$_6$/PCBM, eight optimized geometries of P3MT$_6$/PCBM, frontier orbitals of P3MT$_4$/PCBM and P3MT$_8$/PCBM, and electronic coupling under eight different orientations of P3MT$_6$/PCBM. This material is available free of charge via the Internet at http://pubs.acs.org.

■ AUTHOR INFORMATION

Corresponding Author

*T.L.: e-mail T.Liu.7@warwick.ac.uk. A.T.: e-mail A.Troisi@warwick.ac.uk.

■ ACKNOWLEDGMENT

We are grateful to EPRSC and ERC for supporting this work and to David McMahon for helpful comments on this manuscript.

■ REFERENCES

(1) Green, M. A. *Physica E* **2002,** *14*, 11–17.
(2) Blom, P. W. M.; Mihailetchi, V. D.; Koster, L. J. A.; Markov, D. E. *Adv. Mater.* **2007,** *19*, 1551–1566.
(3) Thompson, B. C.; Frechet, J. M. J. *Angew. Chem. Int. Ed* **2008,** *47*, 58–77.
(4) Yu, G.; Gao, J.; Hummelen, J. C.; Wudl, F.; Heeger, A. J. *Science* **1995,** *270*, 1789–1791.
(5) Halls, J. J. M.; Walsh, C. A.; Greenham, N. C.; Marseglia, E. A.; Friend, R. H.; Moratti, S. C.; Holmes, A. B. *Nature* **1995,** *376*, 498–500.
(6) Ai, X.; Beard, M. C.; Knutsen, K. P.; Shaheen, S. E.; Rumbles, G.; Ellingson, R. J. *J. Phys. Chem. B* **2006,** *110*, 25462–25471.
(7) Hwang, I. W.; Moses, D.; Heeger, A. J. *J. Phys. Chem. C* **2008,** *112*, 4350–4354.
(8) Ohkita, H.; Cook, S.; Astuti, Y.; Duffy, W.; Tierney, S.; Zhang, W.; Heeney, M.; McCulloch, I.; Nelson, J.; Bradley, D. D. C.; Durrant, J. R. *J. Am. Chem. Soc.* **2008,** *130*, 3030–3042.
(9) Kanai, Y.; Grossman, J. C. *Nano Lett.* **2007,** *7*, 1967–1972.
(10) Li, G.; Shrotriya, V.; Huang, J. S.; Yao, Y.; Moriarty, T.; Emery, K.; Yang, Y. *Nat. Mater.* **2005,** *4*, 864–868.
(11) Froves, C. R., O. G.; Ginger, D. S. *Acc. Chem. Res.* **2010,** *43*, 612–620.
(12) Guo, J. M. O., H.; Benten, H.; Ito, S. *J. Am. Chem. Soc.* **2010,** *132*, 6154–6164.
(13) Ma, W. L.; Yang, C. Y.; Gong, X.; Lee, K.; Heeger, A. J. *Adv. Funct. Mater.* **2005,** *15*, 1617–1622.
(14) Choi, J. H.; Son, K. I.; Kim, T.; Kim, K.; Ohkubo, K.; Fukuzumi, S. *J. Mater. Chem.* **2010,** *20*, 475–482.
(15) Wong, W. Y.; Wang, X. Z.; He, Z.; Djurisic, A. B.; Yip, C. T.; Cheung, K. Y.; Wang, H.; Mak, C. S. K.; Chan, W. K. *Nat. Mater.* **2007,** *6*, 521–527.
(16) Chen, H. Y.; Hou, J. H.; Zhang, S. Q.; Liang, Y. Y.; Yang, G. W.; Yang, Y.; Yu, L. P.; Wu, Y.; Li, G. *Nat. Photonics* **2009,** *3*, 649–653.
(17) Peet, J.; Kim, J. Y.; Coates, N. E.; Ma, W. L.; Moses, D.; Heeger, A. J.; Bazan, G. C. *Nat. Mater.* **2007,** *6*, 497–500.
(18) Bijleveld, J. C.; Zoombelt, A. P.; Mathijssen, S. G. J.; Wienk, M. M.; Turbiez, M.; de Leeuw, D. M.; Janssen, R. A. J. *J. Am. Chem. Soc.* **2009,** *131*, 16616–16617.
(19) Liang, Y. Y.; Xu, Z.; Xia, J. B.; Tsai, S. T.; Wu, Y.; Li, G.; Ray, C.; Yu, L. P. *Adv. Mater.* **2010,** *22*, E135–E138.
(20) Brédas, J. L.; Norton, J. E.; Cornil, J.; Coropceanu, V. *Acc. Chem. Res.* **2009,** *42*, 1691–1699.
(21) Deibel, C.; Mack, D.; Gorenflot, J.; Scholl, A.; Krause, S.; Reinert, F.; Rauh, D.; Dyakonov, V. *Phys. Rev. B* **2010,** *81*, 085202.
(22) Jortner, J. *J. Chem. Phys.* **1976,** *64*, 4860–4867.
(23) Marcus, R. A. *Faraday Discuss. Chem. Soc.* **1982,** *74*, 7–15.
(24) Barbara, P. F.; Meyer, T. J.; Ratner, M. A. *J. Phys. Chem.* **1996,** *100*, 13148–13168.
(25) Piris, J.; Dykstra, T. E.; Bakulin, A. A.; van Loosdrecht, P. H. M.; Knulst, W.; Trinh, M. T.; Schins, J. M.; Siebbeles, L. D. A. *J. Phys. Chem. C* **2009,** *113*, 14500–14506.
(26) Ma, W.; Kim, J. Y.; Lee, K.; Heeger, A. J. *Macromol. Rapid Commun.* **2007,** *28*, 1776–1780.
(27) Kawatsu, T.; Coropceanu, V.; Ye, A. J.; Brédas, J. L. *J. Phys. Chem. C* **2008,** *112*, 3429–3433.
(28) Lemaur, V.; Steel, M.; Beljonne, D.; Brédas, J. L.; Cornil, J. *J. Am. Chem. Soc.* **2005,** *127*, 6077–6086.
(29) Yi, Y. P.; Coropceanu, V.; Brédas, J. L. *J. Am. Chem. Soc.* **2009,** *131*, 15777–15783.
(30) Roncali, J. *Chem. Rev.* **1992,** *92*, 711–738.
(31) Liu, T.; Gao, J. S.; Xia, B. H.; Zhou, X.; Zhang, H. X. *Polymer* **2007,** *48*, 502–511.
(32) Goeb, S.; De Nicola, A.; Ziessel, R. *J. Org. Chem.* **2005,** *70*, 1518–1529.
(33) Runge, E.; Gross, E. K. U. *Phys. Rev. Lett.* **1984,** *52*, 997–1000.
(34) Parr, R. G. Y., W. T. *Density functionaltheory of atoms and molecules*; Oxford University Press: New York, 1989.
(35) Becke, A. D. *J. Chem. Phys.* **1993,** *98*, 5648–5652.
(36) Zhao, Y.; Truhlar, D. G. *Acc. Chem. Res.* **2008,** *41*, 157–167.
(37) Dreuw, A.; Head-Gordon, M. *Chem. Rev.* **2005,** *105*, 4009–4037.
(38) Dreuw, A.; Head-Gordon, M. *J. Am. Chem. Soc.* **2004,** *126*, 4007–4016.
(39) Dreuw, A.; Weisman, J. L.; Head-Gordon, M. *J. Chem. Phys.* **2003,** *119*, 2943–2946.
(40) Adamo, C.; Barone, V. *J. Chem. Phys.* **1998,** *108*, 664–675.
(41) Liu, T.; Xia, B. H.; Zhou, X.; Zhang, H. X.; Pan, Q. J.; Gao, J. S. *Organometallics* **2007,** *26*, 143–149.
(42) Liu, T.; Xia, B. H.; Zheng, Q. C.; Zhou, X.; Pan, Q. J.; Zhang, H. X. *J. Comput. Chem.* **2010,** *31*, 628–638.
(43) The background charge method includes polarization to the first order, in the sense that the polarization of each fragment due to the surrounding charge is naturally included in the method. However, the surrounding charge is not modified to take into account the effect of polarization, and so higher order polarization effects are excluded.
(44) Chirlian, L. E.; Francl, M. M. *J. Comput. Chem.* **1987,** *8*, 894–905.
(45) Malagoli, M.; Coropceanu, V.; da Silva, D. A.; Brédas, J. L. *J. Chem. Phys.* **2004,** *120*, 7490–7496.
(46) Della Valle, R. G.; Brillante, A.; Farina, L.; Venuti, E.; Masino, M.; Girlando, A. *Mol. Cryst. Liq. Cryst.* **2004,** *416*, 145–154.
(47) Di Motta, S.; Di Donato, E.; Negri, F.; Orlandi, G.; Fazzi, D.; Castiglioni, C. *J. Am. Chem. Soc.* **2009,** *131*, 6591–6598.
(48) Norton, J. E.; Brédas, J. L. *J. Am. Chem. Soc.* **2008,** *130*, 12377–12384.
(49) McMahon, D. P.; Troisi, A. *J. Phys. Chem. Lett.* **2010,** *1*, 941–946.
(50) Marcus, R. A. *Rev. Mod. Phys.* **1993,** *65*, 599–610.
(51) Burquel, A.; Lemaur, V.; Beljonne, D.; Lazzaroni, R.; Cornil, J. *J. Phys. Chem. A* **2006,** *110*, 3447–3453.
(52) Marcus, R. A. *J. Chem. Phys.* **1965,** *24*, 966–978.
(53) Marcus, R. A.; Sutin, N. *Biochim. Biophys. Acta* **1985,** *811*, 265–322.

(54) Marcus, R. A. *Annu. Rev. Phys. Chem.* **1964,** *15*, 155–196.
(55) German, E. D.; Kuznetsov, A. M. *Electrochim. Acta* **1981,** *26*, 1595–1608.
(56) German, E. D.; Kharkats, Y. I. *Chem. Phys. Lett.* **1995,** *245*, 427–430.
(57) Sharp, K. A. *Biophys. J.* **1998,** *73*, 1241–1250.
(58) Troisi, A.; Ratner, M. A.; Zimmt, M. B. *J. Am. Chem. Soc.* **2004,** *126*, 2215–2224.
(59) Voityuk, A. A.; Rösch, N. *J. Chem. Phys.* **2002,** *117*, 5607–5616.
(60) Cave, R. J.; Newton, M. D. *Chem. Phys. Lett.* **1996,** *249*, 15–19.
(61) Wu, Q.; Van Voorhis, T. *Phys. Rev. A* **2005,** *72*, 024502.
(62) Hsu, C.-P. *Acc. Chem. Res.* **2009,** *42*, 509–518.
(63) Yeganeh, S.; Van Voorhis, T. *J. Phys. Chem. C* **2010**, DOI: 10.1021/jp106989t.
(64) Huang, J.; Kertesz, M. *Chem. Phys. Lett.* **2004,** *390*, 110–115.
(65) Huang, J.; Kertesz, M. *J. Chem. Phys.* **2005,** *122*, 234707.
(66) Frisch, M. J.; Trucks, G. W.; Schlegel, H. B.; Scuseria, G. E.; Robb, M. A.; Cheeseman, J. R.; Montgomery, J. A., Jr.; Vreven, T.; Kudin, K. N.; Burant, J. C.; Millam, J. M.; Iyengar, S. S.; Tomasi, J.; Barone, V.; Mennucci, B.; Cossi, M.; Scalmani, G.; Rega, N.; Petersson, G. A.; Nakatsuji, H.; Hada, M.; Ehara, M.; Toyota, K.; Fukuda, R.; Hasegawa, J.; Ishida, M.; Nakajima, T.; Honda, Y.; Kitao, O.; Nakai, H.; Klene, M.; Li, X.; Knox, J. E.; Hratchian, H. P.; Cross, J. B.; Adamo, C.; Jaramillo, J.; Gomperts, R.; Stratmann, R. E.; Yazyev, O.; Austin, A. J.; Cammi, R.; Pomelli, C.; Ochterski, J. W.; Ayala, P. Y.; Morokuma, K.; Voth, G. A.; Salvador, P.; Dannenberg, J. J.; Zakrzewski, V. G.; Dapprich, S.; Daniels, A. D.; Strain, M. C.; Farkas, O.; Malick, D. K.; Rabuck, A. D.; Raghavachari, K.; Foresman, J. B.; Ortiz, J. V.; Cui, Q.; Baboul, A. G.; Clifford, S.; Cioslowski, J.; Stefanov, B. B.; Liu, G.; Liashenko, A.; Piskorz, P.; Komaromi, I.; Martin, R. L.; Fox, D. J.; Keith, T.; Al-Laham, M. A.; Peng, C. Y.; Nanayakkara, A.; Challacombe, M.; Gill, P. M. W.; Johnson, B.; Chen, W.; Wong, M. W.; Gonzalez, C.; Pople, J. A. *Gaussian 03*; Gaussian, Inc.: Wallingford, CT, 2004.
(67) Duskesas, G.; Larsson, S. *Theor. Chem. Acc.* **1997,** *97*, 110–118.
(68) Zhang, C. R.; Chen, H. S.; Chen, Y. H.; Wei, Z. Q.; Pu, Z. S. *Acta Phys.-Chim. Sin.* **2008,** *24*, 1353–1358.
(69) Horowitz, G.; Bachet, B.; Yassar, A.; Lang, P.; Demanze, F.; Fave, J.-L.; Garnier, F. *Chem. Mater.* **1995,** *7*, 1337–1341.
(70) Barbarella, G.; Zambianchi, M.; Bongini, A.; Antolini, L. *Adv. Mater.* **1994,** *4*, 282–285.
(71) Yassar, A.; Garnier, F.; Deloffre, F.; Horowitz, G.; Ticard, L. *Adv. Mater.* **1994,** *6*, 660–663.
(72) Lap, D. V.; Grebner, D.; Rentsch, S. *J. Phys. Chem. A* **1997,** *101*, 107–112.
(73) Ran, X. Q.; Feng, J. K.; Ren, A. M.; Tian, W. Q.; Zou, L. Y.; Liu, Y. L.; Sun, C. C. *J. Phys. Org. Chem.* **2009,** *22*, 680–690.
(74) Darling, S. B. *J. Phys. Chem. B* **2008,** *112*, 8891–8895.
(75) Schueppel, R.; Uhrich, C.; Pfeiffer, M.; Leo, K.; Brier, E.; Reinold, E.; Baeuerle, P. *ChemPhysChem* **2007,** *8*, 1497–1503.
(76) Deibel, C.; Dyakonov, V. *Rep. Prog. Phys.* **2010,** *73*, 096401.
(77) Dyer-Smith, C.; Reynolds, L. X.; Bruno, A.; Bradley, D. D. C.; Haque, S. A.; Nelson, J. *Adv. Funct. Mater.* **2010,** *20*, 2701–2708.
(78) Cohen, A. J.; Mori-Sánchez, P.; Yang, W. *J. Chem. Phys.* **2008,** *129*, 121104.
(79) Banerji, N.; Furstenberg, A.; Bhosale, S.; Sisson, A. L.; Sakai, N.; Matile, S.; Vauthey, E. *J. Phys. Chem. B* **2008,** *112*, 8912–8922.
(80) Lee, J.; Vandewal, K.; Yost, S. R.; Bahlke, M. E.; Goris, L.; Baldo, M. A.; Manca, J. V.; Van Voorhis, T. *J. Am. Chem. Soc.* **2010,** *132*, 11878–11880.
(81) Clarke, T.; Ballantyne, A.; Jamieson, F.; Brabec, C.; Nelson, J.; Durrant, J. *Chem. Commun.* **2009,** 89–91.
(82) Weller, A. Z. *Phys. Chem. Neue Folge* **1982,** *133*, 93–98.
(83) Vandewal, K. T., K.; Gadisa, A; Inganas, O.; Manca, J. V. *Phy. Rev. B* **2010,** *81*, 125204.
(84) Bader, R. F. W.; Preston, H. J. T. *Theor. Chim. Acta* **1970,** *17*, 384–395.
(85) Bader, R. F. W.; Carroll, M. T.; Cheeseman, J. R.; Chang, C. *J. Am. Chem. Soc.* **1987,** *109*, 7968–7979.
(86) Koster, L. J. A.; Mihailetchi, V. D.; Blom, P. W. M. *Appl. Phys. Lett.* **2006,** *88*, 093511.
(87) Glatthaar, M.; Riede, M.; Keegan, N.; Sylvester-Hvid, K.; Zimmermann, B.; Niggemann, M.; Hinsch, A.; Gombert, A. *Sol. Energy Mater. Sol. Cells* **2007,** *91*, 390–393.
(88) Hoppe, H.; Shokhovets, S.; Gobsch, G. *Phys. Stat. Sol. (RRL)* **2007,** *1*, R40–R42.
(89) Moule, A. J.; Meerholz, K. *Appl. Phys. Lett.* **2007,** *91*, 061901.
(90) Hamnett, A.; Hillman, A. R. *J. Electrochem. Soc.* **1988,** *135*, 2517–2524.
(91) Cheung, D. L.; McMahon, D. P.; Troisi, A. *J. Am. Chem. Soc.* **2009,** *131*, 11179–11186.
(92) Cheung, D. L.; Troisi, A. *J. Phys. Chem. C* **2010**, DOI: 10.1021/jp1049167.
(93) Grzegorczyk, W. J.; Savenije, T. J.; Dykstra, T. E.; Piris, J.; Schins, J. M.; Siebbeles, L. D. A. *J. Phys. Chem.* **2010,** *114*, 5182–5186.
(94) Braun, S.; Salaneck, W. R.; Fahlman, M. *Adv. Mater.* **2009,** *21*, 1450–1472.
(95) Avilov, I.; Geskin, V.; Cornil, J. *Adv. Funct. Mater.* **2009,** *19*, 624–633.
(96) Vásquez, H.; Flores, F.; Oszwaldowski, R.; Ortega, J.; Pérez, R.; Kahn, A. *Appl. Surf. Sci.* **2004,** *234*, 107–112.
(97) Alcamí, M.; Mó, O.; Yáñez, M. *Mass Spectrom. Rev.* **2001,** *20*, 195–245.
(98) Sousa, S. F.; Fernandes, P. A.; Ramos, M. J. *J. Phys. Chem. A* **2007,** *111*, 10439–10452.
(99) Vukmirovic, N.; Wang, L. W. *Nano Lett.* **2009,** *9*, 3996–4000.
(100) Prins, P.; Grozema, F. C.; Galbrecht, F.; Scherf, U.; Siebbeles, L. D. A. *J. Phys. Chem. C* **2007,** *111*, 11104–11112.
(101) Olivier, Y.; Muccioli, L.; Lemaur, V.; Geerts, Y. H.; Zannoni, C.; Cornil, J. *J. Phys. Chem. B* **2009,** *113*, 14102–14111.
(102) Marcon, V.; Breiby, D. W.; Pisula, W.; Dahl, J.; Kirkpatrick, J.; Patwardhan, S.; Grozema, F.; Andrienko, D. *J. Am. Chem. Soc.* **2009,** *131*, 11426–11432.
(103) Kubar, T.; Kleinekathofer, U.; Elstner, M. *J. Phys. Chem. B* **2009,** *113*, 13107–13117.